Proceedings of FEDSM2005
2005 ASME Fluids Engineering Division Summer Meeting and Exhibition
June 19-23, 2005, Houston, TX, USA

FEDSM2005-77476

ANALYSIS OF TWO-PHASE SUPERSONIC FLOW IN JET PUMPS

S.M. Kandil
W.E. Lear
S.A. Sherif
Department of Mechanical and Aerospace Engineering
University of Florida
P.O. Box 116300
Gainesville, FL, 32611-6300
Tel: (352) 392-7821, Fax: (352) 392-1071, Email: sasherif@ufl.edu

ABSTRACT

A jet pump may be constructed from a pair of concentric tubes in which the center tube is shaped as a converging-diverging nozzle. Primary fluid is allowed to accelerate through the nozzle, thus creating a low-pressure region at the nozzle exit. Secondary fluid flowing in the peripheral region is drawn into the low-pressure region and is thus accelerated. In this study, the jet pump is employed as part of a space thermal-management system based on a cycle known as the Solar Integrated Thermal Management and Power (SITMAP). The latter is a combined vapor compression cycle and a Rankine cycle with the compression device being a jet pump instead of the regular compressor. The jet pump has several advantages for space applications as it involves no moving parts, a feature that results in decreasing the weight and vibration level while increasing the system reliability. The working fluid is cryogenic nitrogen, which is readily present onboard the spacecraft. This study presents a detailed component analysis of the jet pump allowing for two-phase supersonic flow. The model also accounts for Fabri choking either at the inlet or at an aerodynamic throat in the mixing chamber. The model also accounts for flow choking at the exit of the mixing chamber. The different choking situations limit the ability of the jet pump to entrain more secondary flow once the flow is choked at any location. In this study the various choking regimes will be identified and the entrainment ratios corresponding to the different choking scenarios will be calculated.

NOMENCLATURE

Latin Symbols

A	cross-sectional area, m^2
a	speed of sound, m/s
h	specific enthalpy, kJ/kg
M	Mach number, dimensionless
m	mass, kg
$\dot{m}$	mass flow rate, kg/s
P	pressure, MPa
P_r	compression ratio
T	temperature, ^oC
V	velocity, m/s

Greek Symbols

ϕ	entrainment ratio, $\dot{m}_s / \dot{m}_p$
ρ	density, kg/m^3

Subscripts

R	refrigeration
T	total
de	diffuser exit
ei	evaporator inlet
evap	evaporator
me	mixing chamber exit
n2	primary flow passage where Fabri choking occurs
ne	primary nozzle exit
nt	primary nozzle throat
p	primary flow
pi	primary nozzle inlet
pe	pump exit
s2	secondary flow passage where Fabri choking occurs
s	secondary flow
se	secondary flow exit
si	secondary flow inlet
ss	state immediately downstream of shock wave

INTRODUCTION

A jet pump is conceptually a pair of concentric tubes in which usually the center tube consists of a nozzle of a high-pressure jet of fluid. The jet pump, if used as a compression device in place of the compressor in a space-based vapor compression refrigeration system, can have several advantages

as it involves no moving parts, which decreases the weight and vibration level while increasing the reliability.

Due to their design simplicity, jet pumps (see Figure 1) are widely used in many applications such as pumping, mixing, and entrainment. They are also used in a myriad of industries such as vacuum packaging (vacuum pumps), oil drilling, thrust augmentation in turbine jet engines, and ejector-compression heat pumps. In most applications ejectors are made of two concentric and coaxial nozzles. A high-pressure flow (primary flow) is accelerated to supersonic speed which entrains the low-pressure fluid (secondary flow) by means of viscous interactions. The two streams mix in a constant-area mixing tube. The entrainment ratio is defined as the ratio between the secondary mass flow-rate to the primary mass flow-rate. Under certain conditions when the pressure P_{ne} is greater than P_{se} the primary flow expands into the mixing chamber creating an aerodynamic throat that constricts the area available for the secondary flow. This causes the secondary flow to accelerate, sometimes reaching sonic speed. When this happens the secondary flow is then choked, thus the secondary mass flow rate cannot be increased anymore. This phenomenon is referred to as Fabri choking, and it limits the value of the entrainment ratio that can be achieved for given inlet conditions and jet-pump geometry.

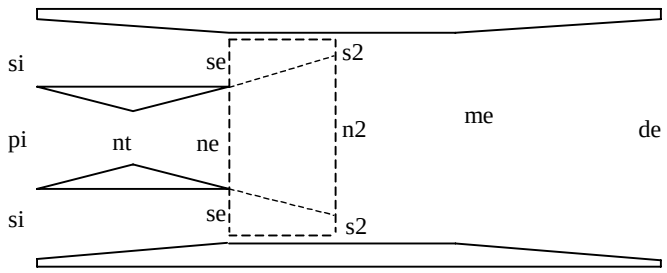

Figure 1. Schematic of the jet-pump with constant-area mixing

The Fabri choking phenomenon was first introduced by Fabri and Paulon (1958) and Fabri and Siestrunk (1958). Both studies involved supersonic air ejectors. They divided the operation of the supersonic ejector into three regimes, namely, the supersonic regime, the saturated supersonic regime, and the mixed regime. The supersonic regime refers to the operating conditions when the primary flow pressure at the inlet is larger than the secondary flow pressure ($P_{ne} > P_{se}$) which causes the primary flow to expand into the secondary flow, as indicated by the dotted line in Figure 1. This causes the secondary flow to choke in an aerodynamic throat ($M_{s2} = 1$) in the mixing chamber. The saturated supersonic regime is a limiting case of the supersonic flow regime, where the P_{si} increases and the secondary flow chokes at the inlet to the mixing chamber ($M_{se} = 1$). In both these flow regimes, once the flow is choked either at "se" or "s2", the entrainment ratio becomes independent of the downstream flow. The third regime is basically the regime before the flow reaches one of the choked regimes. In the mixed flow regime the entrainment ratio is dependent on the upstream and downstream conditions.

In this study a comprehensive one-dimensional flow model is developed and coded for the jet-pump analysis. The model assumes the jet-pump to be operating at the Fabri limit (breakoff) where the entrainment ratio becomes independent of the compression ratio due to choking of the secondary stream at either the inlet or at an aerodynamic throat location near the inlet. Another very important phenomenon that was discovered by Dutton and Carroll (1988) is the exit flow choking at the mixing chamber exit. Dutton and Carroll observed the phenomenon for ejectors operation with perfect gases, however the same phenomenon was observed in our study with liquid nitrogen as the working fluid. In some cases no solution was found for the mixed state at "me" with the entrainment ratio at the "breakoff" or the Fabri limit. The entrainment ratio was lowered until a converged solution was found for the mixed state, at which the mixed state Mach number was unity. Thus, even though it is possible to find the inlet conditions at the Fabri breakoff point, since they are based on separate control volume relations written between "ne", "se" and "n2", "s2", no mixed state solution at "me" is possible for these inlet conditions. This phenomenon is referred to as exit choking which imposes another constraint on the limit for the entrainment ratio. In this study the various choking regimes will be identified and the entrainment ratios corresponding to the different choking scenarios will be calculated. The working fluid employed is cryogenic nitrogen, which is readily present onboard spacecraft.

MATHEMATICAL MODEL

First, it should be noted that the inputs to the jet-pump simulation code are:

- The temperature and pressure at the jet-pump primary inlet state, P_{pi}, and T_{pi}.
- The temperature and pressure at the jet-pump secondary inlet state, P_{si}, and T_{si}.
- Primary nozzle area ratio A_{nt}/A_{ne}.
- Secondary-to-primary area ratio, A_{ne}/A_{se}.

The complete method for calculating the diffuser exit state and the entrainment ratio, ϕ, given the jet pump geometry and the primary and secondary inlet states is shown next.

Primary nozzle: To obtain the properties at the nozzle throat "nt", P_{nt} is guessed and since isentropic flow is assumed, $s_{nt} = s_{pi}$. The following conservation equations are used, and P_{nt} is iterated till M_{nt} is equal to unity.

$$V_{pi} = \frac{\rho_{nt}}{\rho_{pi}} \frac{A_{nt}}{A_{pi}} V_{nt} \qquad \textbf{(1)}$$

$$V_{nt} = \left[\frac{h_{pi} - h_{nt}}{\frac{1}{2}\left[1 - \left(\frac{\rho_{nt}}{\rho_{pi}}\frac{A_{nt}}{A_{pi}}\right)^2\right]} \right]^{\frac{1}{2}} \quad \textbf{(2)}$$

All Mach numbers throughout this analysis are calculated using Equations (3) and (4). The 's' in Equation (3) signifies an isentropic process

$$a = \sqrt{\left(\frac{dP}{d\rho}\right)_s} \quad \textbf{(3)}$$

$$M = \frac{V}{a} \quad \textbf{(4)}$$

The properties at the nozzle exit "ne" are obtained by the assumption of isentropic flow, $s_{ne}=s_{nt}$, and guessing P_{ne} using the following conservation equations

$$V_{ne} = \left[2\left(h_{nt} + \frac{1}{2}V_{nt}^2 - h_{ne} \right) \right]^{\frac{1}{2}} \quad \textbf{(5)}$$

$$\frac{A_{nt}}{A_{ne}} = \frac{\rho_{ne}}{\rho_{nt}}\frac{V_{ne}}{V_{nt}} \quad \textbf{(6)}$$

P_{ne} is iterated till A_{nt}/A_{ne} matches its input value.

Flow choking analysis:

The flow choking analysis is comprised of three parts corresponding to the three different choking conditions for the flow in the mixing chamber of the jet-pump. There are three different values for the entrainment ratio corresponding to the three choking conditions. The minimum of these three values is the maximum entrainment ratio that can be achieved for a given primary and secondary inlet conditions and a given geometry. The first place where the flow can choke is at (se), refer to Figure 1. This happens when the backpressure drops and V_{se} reaches sonic velocity. This flow regime is referred to as the "Saturated Supersonic Regime." To calculate ϕ corresponding to these conditions, iterations are done on P_{se} till it reaches the critical pressure corresponding to the given stagnation pressure, P_{si}. Then $\phi_{inlet,choke}$ is calculated from its definition as

$$\phi_{inletchoke} = \frac{\rho_{se}V_{se}A_{se}}{\rho_{ne}V_{ne}A_{ne}} \quad \textbf{(7)}$$

The second choking possibility, as discussed by Fabri et al. (1958), is when the back-pressure is not low enough to cause choking at (se), but is low enough to cause P_{se} to be less than P_{ne}. This regime is referred to as the "Supersonic Regime." In this case the primary flow expands in the mixing chamber constricting the available flow area for the secondary stream, causing it to accelerate. It is possible for the secondary stream to reach sonic speed at an aerodynamic throat, thus causing the secondary mass flow rate to become independent of downstream conditions.

The following analysis is used to calculate ϕ_{Fabri}. The momentum equation for the control volume shown in Figure 1 can be written as

$$\phi_{Fabri} = \frac{\left(P_{se} + P_{ne}\frac{A_{ne}}{A_{se}} - P_{s2}\frac{A_{s2}}{A_{se}} - P_{n2}\frac{A_{n2}}{A_{ne}}\frac{A_{ne}}{A_{se}} \right)}{\rho_{ne}V_{ne}\frac{A_{ne}}{A_{se}}\left(V_{s2} - V_{se}\right)} - \frac{\left(V_{n2} - V_{ne}\right)}{\left(V_{s2} - V_{se}\right)} \quad \textbf{(8)}$$

The iteration scheme starts by guessing a value for P_{se}, knowing that $s_{se} = s_{si}$, this defines the state (se). From the energy equation

$$V_{se} = \left[2\left(h_{si} - h_{se}\right) \right]^{1/2} \quad \textbf{(9)}$$

then ϕ_{Fabri} can be calculated as

$$\phi_{Fabri} = \frac{\rho_{se}V_{se}A_{se}}{\rho_{ne}V_{ne}A_{ne}} \quad \textbf{(10)}$$

It should be noted that the area ratio A_{ne}/A_{se} is an input to the code. Then a guess is made for P_{s2}, and $s_{s2} = s_{se}$, that defines the state (s2). The following conservation equation is used

$$V_{s2} = \left[2\left(h_{se} - h_{s2} + \frac{V_{se}^2}{2} \right) \right]^{1/2} \quad \textbf{(11)}$$

Calculate $M_{s2} = \frac{V_{s2}}{a_{s2}}$, and check if it is equal to 1. If not another value for P_{s2} is guessed till $M_{s2} = 1$.

The area ratio A_{s2}/A_{se} can be calculated from the continuity equation between se and s2,

$$\frac{A_{s2}}{A_{se}} = \frac{\rho_{se}V_{se}}{\rho_{s2}V_{s2}} \quad \textbf{(12)}$$

Knowing that for constant-area mixing $A_{ne} + A_{se} = A_{s2} + A_{n2}$, then

$$\frac{A_{n2}}{A_{ne}} = 1 + \frac{A_{se}}{A_{ne}} - \left(\frac{A_{s2}}{A_{se}}\frac{A_{se}}{A_{ne}} \right) \quad \textbf{(13)}$$

From Equation (8) another value for ϕ_{Fabri} can be obtained. Iterate on P_{se} till the values for ϕ_{Fabri} from Equations (8) and (10) match.

The third limit on the maximum entrainment ratio is when the flow chokes at the mixing chamber exit, state (me). As mentioned before, this flow scenario was observed when no converged mixed state solution was found for some values of ϕ_{Fabri}, and $\phi_{inletchoke}$. In this case the value of the entrainment ratio was incrementally decreased till a mixed state was found. It was noticed that for this mixed state the Mach number was very close to one. This value of the entrainment ratio is referred to as $\phi_{exitchoke}$. The exit choked condition was rarely encountered in the range of operation investigated so far.

The transition between the "supersonic" and the "saturated supersonic" regimes depends on the stagnation pressure ratio, P_{pi}/P_{si}. There is break-off value for this pressure ratio below which the entrainment ratio upper bound will be that of the "saturated supersonic" regime, and above which the entrainment ratio upper bound will be that of the "supersonic" regime. For a given P_{pi} and jet pump geometry, the break-off pressure ratio is calculated finding the P_{si} that would yield the primary and secondary pressures at the inlet of the mixing chamber to be equal (P_{se}=P_{ne}). The break-off pressure ratio is referred to as $\left(P_{pi}/P_{si}\right)_{bo}$. After calculating the values for all possible upper limits on the entrainment ratio, the maximum possible ϕ is calculated as

$$\phi_{\max} = Min\left(\phi_{inletchoke}, \phi_{exitchoke}\right) \quad \textbf{(14a)}$$

for the "saturated supersonic" regime

$$\phi_{\max} = Min\left(\phi_{Fabri}, \phi_{exitchoke}\right) \quad \textbf{(14b)}$$

for the "supersonic" regime

Mixing chamber:

Again if the value of ϕ input to the analysis is less than the minimum entrainment ratio specified by the choking analysis (i.e. when the jet-pump is operating in the mixed regime), the following analysis is used to calculate state (me). This analysis is similar to that used to calculate $\phi_{exitchoke}$. A guess is made for P_{se}, and since $s_{se} = s_{si}$,, then state (se) is fully specified. The velocity at the secondary exit is calculated using conservation of energy

$$V_{se} = \left[2\left(h_{si} + \frac{1}{2}V_{si}^2 - h_{se}\right)\right]^{\frac{1}{2}} \quad \textbf{(15)}$$

A guess is now made for P_{me} and the momentum equation for the entire mixing chamber, Equation (27), is used to calculate V_{me}. The momentum equation can be written and rearranged as

$$V_{me} = \frac{\left(P_{ne} - P_{me}\right)\frac{A_{ne}}{A_{se}} - \left(P_{se} - P_{me}\right) + \rho_{ne}V_{ne}^2\frac{A_{ne}}{A_{se}} + \rho_{se}V_{se}^2}{\left(1+\phi\right)\rho_{ne}V_{ne}\frac{A_{ne}}{A_{se}}} \quad \textbf{(16)}$$

Then the enthalpy h_{me} is calculated from the energy equation for the mixing chamber

$$h_{me} = \frac{1}{1+\phi}\left[\left(h_{ne} + \frac{1}{2}V_{ne}^2\right) + \phi\left(h_{se} + \frac{1}{2}V_{se}^2\right)\right] - \frac{1}{2}V_{me}^2 \quad \textbf{(17)}$$

P_{me}, and h_{me} completely define state (me). Then $\phi_{exitchoke}$ is recalculated from

$$\phi = \frac{\rho_{me}A_{me}V_{me}}{\rho_{ne}A_{ne}V_{ne}} - 1 \quad \textbf{(18)}$$

P_{me} is iterated till the value of ϕ from Equation (17) matches its input value. Then the mixing chamber exit Mach number is calculated using Equations (3) and (4).

Diffuser:

In case the mixing chamber exit flow is supersonic a shock is assumed to exist at the diffuser inlet where the Mach number is closest to unity and, thus, the stagnation pressure loss over the shock is minimized.

If $M_{me} > 1$, P_{ss} is guessed and Equations (19) through (22) are applied across the shock

$$\rho_{me}V_{me} = \rho_{ss}V_{ss} \quad \textbf{(19)}$$

$$P_{me} + \rho_{me}V_{me}^2 = P_{ss} + \rho_{ss}V_{ss}^2 \quad \textbf{(20)}$$

$$h_{me} + \frac{1}{2}V_{me}^2 = h_{ss} + \frac{1}{2}V_{ss}^2 \quad \textbf{(21)}$$

$$\rho_{ss} = \rho\left(P_{ss}, h_{ss}\right) \quad \textbf{(22)}$$

Equations (19) and (20) can be combined to obtain the velocity downstream of the shock.

$$V_{ss} = \frac{P_{me} + \rho_{me}V_{me}^2 - P_{ss}}{\rho_{me}V_{me}} \quad \textbf{(23)}$$

Equation (23) can be combined with Equation (19) to obtain the density downstream of the shock. Equation (23) can also be used with Equation (21) to obtain the specific enthalpy downstream of the shock, which can be used with Equation (22) to obtain the density downstream of the shock. Iterate on P_{ss} until the density obtained from Equation (19) matches that from Equation (22). To obtain the diffuser exit state for the case of $M_{me} > 1$, follow the procedure for the case when M_{me} is less than or equal to 1, replacing the subscript 'me' with 'ss.'

If $M_{me} \le 1$, then to obtain the properties at the diffuser exit, P_{de} is guessed and the flow assumed to be isentropic (s_{de} = s_{me}). The diffuser exit velocity is calculated using the continuity equation

$$V_{de} = \frac{\rho_{me}}{\rho_{de}}\frac{A_{me}}{A_{ne}}\frac{A_{ne}}{A_{de}}V_{me} \quad \textbf{(24)}$$

The velocity at the diffuser exit is calculated using conservation of energy

$$V_{de} = \left[2\left(h_{me} + \frac{1}{2} V_{me}^2 - h_{de} \right) \right]^{\frac{1}{2}} \quad \textbf{(25)}$$

P_{de} is iterated until the continuity equation and conservation of energy yield the same diffuser exit velocity. Then the Mach number at the diffuser exit is calculated using Equations (3) and (4). The above jet pump analysis is general and applies to all flow regimes, including two-phase flows.

RESULTS AND DISCUSSION

Results of the preceding analysis are presented in Tables 1 through 5. Each of the five sets has the same primary inlet pressure, while varying the secondary pressure. The ratio $\left(P_{pi}/P_{si}\right)_{bo}$ is the break-off pressure ratio. This is the ratio below which the flow operates either in the mixed regime or in the saturated supersonic regime (inlet choking regime), and above which the flow operates either in the mixed regime or the supersonic regime (Fabri choking regime).

There are some general trends that can be seen in all data sets. First, once the pressure ratio P_{pi}/P_{si} is larger than its break-off value, ϕ_{Fabri} becomes the upper limit (supersonic flow regime). When P_{pi}/P_{si} is less than its break-off value the limiting value for the entrainment ratio is $\phi_{inlet\ choke}$ (saturated supersonic regime). For any line of data in all data sets, if the entrainment ratio drops below the limiting value, the jet-pump will be operating in the "mixed regime," where ϕ is dependent on the downstream conditions (or the back pressure). It should also be noted that as long as the ratio P_{pi}/P_{si} is above the break-off ratio, the pressure ratio P_{se}/P_{ne} drops below unity, which is important for the primary flow to expand into the secondary causing Fabri choking to take place.

The second general trend is the increase of the limiting value of the entrainment ratio with higher secondary pressure. This should be expected because since the primary inlet pressure is fixed, a higher secondary stagnation pressure corresponds to a lower backpressure. The lower backpressure allows for more secondary flow entrainment before choking occurs.

Data sets 1 to 3 show the effect of the ratio of primary and secondary stagnation temperatures on the maximum entrainment ratio. Figure 2 is a graphical representation of Tables 1 to 3. It can be seen that higher entrainment ratios can be achieved for higher stagnation temperature ratios. The effect of T_{pi}/T_{si} on maximum ϕ is less significant at higher P_{pi}/P_{si} ratios, but the same trend still holds.

Tables 3 and 4 show the effect of varying the primary nozzle geometry. Figure 3 shows the same effect in graphical form. It can be seen that lower A_{nt}/A_{ne} ratios (i.e. higher M_{ne}) allow more secondary flow entrainment. This makes sense, since the entrainment mechanism is by viscous interaction between the secondary and primary streams. Therefore, faster primary flow should be able to entrain more secondary flow.

Tables 4 and 5 show the effect of the area ratio A_{ne}/A_{se}. Figure 4 shows that lower primary-to-secondary area ratios allow for more entrainment. This trend is expected since a lower area ratio means more area for the secondary flow and thus more secondary mass flow rate. Figure 5 shows the variation of the compression ratio with P_{pi}/P_{si}, for different jet-pump geometries. The compression ratio was calculated for maximum allowable entrainment ratio. It can be seen that as the ratio P_{pi}/P_{si} increases the compression ratio increases as well, which is expected.

Table 1: Data set # 1. T_{pi} = 200, T_{si} = 100, A_{nt}/A_{ne} = 0.25, A_{ne}/A_{se} = 0.1

Ppi	Psi	Ppi / Psi	PHIinlet	PHIfabri	Pse	Pse/Pne	(Ppi / Psi)bo	Pne
3200000	1600000	2	144.996		752031.170	7.30495	16.51	102948
3200000	1066666.667	3	85.465		766654.157	7.447		**Mne**
3200000	640000	5	11.1029		366170.684	3.55685		3.07605
3200000	320000	10	5.58389		169866.433	1.65002		
3200000	213333.3333	15	3.67901		113017.917	1.09781		
3200000	160000	20		2.683032	100556.41	0.97677		
3200000	128000	25		2.083661	86249.331	0.83779		
3200000	106666.6667	30		1.676613	76063.5258	0.73885		
3200000	91428.57143	35		1.383796	68217.1583	0.66264		
3200000	80000	40		1.164268	61920.2561	0.60147		
3200000	71111.11111	45		0.9936368	56761.0127	0.55136		
3200000	64000	50		0.8574538	52445.6223	0.50944		

Table 2: Data set # 2. T_{pi} = 100, T_{si} = 100, A_{nt}/A_{ne} = 0.25, A_{ne}/A_{se} = 0.1

Ppi	Psi	Ppi / Psi	PHIinlet	PHIfabri	Pse	Pse/Pne	(Ppi / Psi)bo	Pne
3200000	1600000	2	23.2413		752031.17	1.8963	4.62411	396579
3200000	1066666.667	3	13.6961		766654.081	1.93317		**Mne**
3200000	533333.3333	6		1.416579	376543.452	0.94948		2.57789
3200000	320000	10		0.6935064	264842.461	0.66782		
3200000	213333.3333	15		0.3329346	195893.323	0.49396		

Table 3: Data set # 3. T_{pi} = 400, T_{si} = 100, A_{nt}/A_{ne} = 0.25, A_{ne}/A_{se} = 0.1

P_{pi}	P_{si}	P_{pi}/P_{si}	$\phi_{inletchoke}$	ϕ_{Fabri}	ϕ	P_{se}/P_{ne}	P_{de}/P_{si}	$(P_{de}/P_{si})_{bo}$	P_{ne}
3200000	1600000.000	2	213.904		213.904	7.968	0	18.009699	94375.5814
3200000	640000.000	5	16.3609		16.36093	3.880	1.0485		M_{ne}
3200000	320000.000	10	8.22779		8.227792	1.800	1.19303		2.957
3200000	213333.333	15	5.42427		5.424266	1.198	1.34552		
3200000	160000.000	20		3.9997	3.999688	0.878	1.49797		
3200000	128000.000	25		3.1214	3.121448	0.773	1.65079		
3200000	106666.667	30		2.5321	2.532101	0.691	1.80439		
3200000	91428.571	35		2.1111	2.111098	0.627	1.95876		
3200000	80000.000	40		1.7958	1.795751	0.574	2.11383		
3200000	71111.111	45		1.5509	1.55091	0.543	2.26951		
3200000	64000.000	50		1.359	1.359	0.529	2.427		

Table 4: Data set # 4. T_{pi} = 400, T_{si} = 100, A_{nt}/A_{ne} = 0.6, A_{ne}/A_{se} = 0.1

P_{pi}	P_{si}	P_{pi}/P_{si}	$\phi_{inletchoke}$	ϕ_{Fabri}	ϕ	P_{se}/P_{ne}	P_{de}/P_{si}	$(P_{de}/P_{si})_{bo}$	P_{ne}
3200000	1600000.000	2	89.060			1.816	0.637	4.433	414056.656
3200000	640000.000	5		6.738	6.704	0.995	1.187		M_{ne}
3200000	320000.000	10		3.052	3.052	0.575	1.508		1.996
3200000	213333.333	15		1.810	1.810	0.420	1.842		
3200000	160000.000	20		1.194	1.194	0.334	2.183		
3200000	128000.000	25		0.832	0.832	0.278	2.527		
3200000	106666.667	30		0.594	0.594	0.239	2.876		
3200000	91428.571	35		0.428	0.428	0.210	3.228		
3200000	80000.000	40		0.305	0.305	0.187	3.583		
3200000	71111.111	45		0.2109	0.210895	0.165	3.941		
3200000	64000.000	50		0.137	0.137	0.153	4.301		

Table 5: Data set # 5. T_{pi} = 400, T_{si} = 100, A_{nt}/A_{ne} = 0.25, A_{ne}/A_{se} = 0.3

P_{pi}	P_{si}	P_{pi}/P_{si}	$\phi_{inletchoke}$	ϕ_{Fabri}	ϕ	P_{se}/P_{ne}	P_{de}/P_{si}	$(P_{de}/P_{si})_{bo}$	P_{ne}
3200000	1600000.000	2	71.301		71.301	7.968	0.715	18.009699	94375.581
3200000	640000.000	5	5.459		5.459	3.876	1.131		M_{ne}
3200000	320000.000	10	2.745		2.745	1.800	1.658		2.957
3200000	213333.333	15	1.810		1.810	1.198	2.185		
3200000	160000.000	20		1.008	1.008	1.112	2.712		
3200000	128000.000	25		0.789	0.789	0.942	3.108		
3200000	106666.667	30		0.631	0.631	0.850	3.507		
3200000	91428.571	35		0.513	0.513	0.772	3.908		
3200000	80000.000	40		0.421	0.421	0.706	4.311		
3200000	71111.111	45		0.401	0.401	0.650	4.561		
3200000	64000.000	50		0.348	0.348	0.602	4.716		

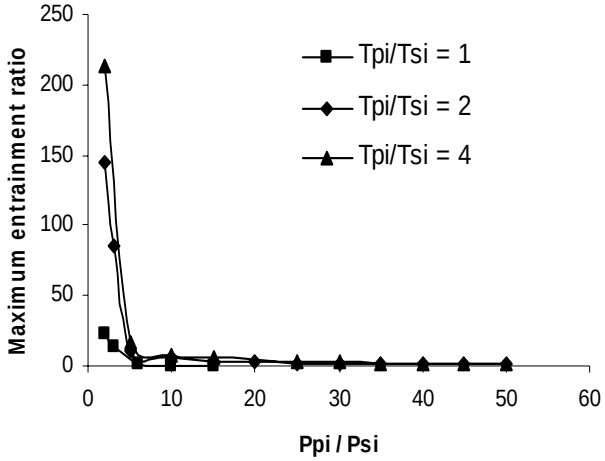

Figure 2: Maximum entrainment ratio variation versus the stagnation pressure ratio for different stagnation temperature ratios (based on $\phi_{inletchoke}$ and ϕ_{Fabri} only)

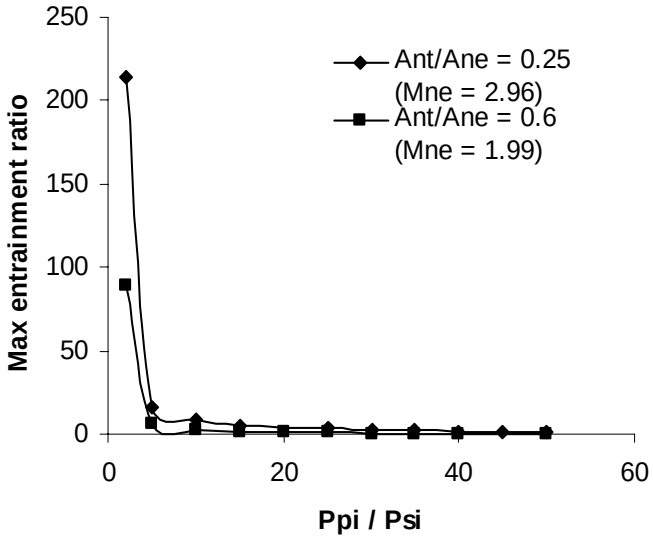

Figure 3: Maximum entrainment ratio variation versus the stagnation pressure ratio for different primary nozzle geometry (based on $\phi_{inletchoke}$, and ϕ_{Fabri} only)

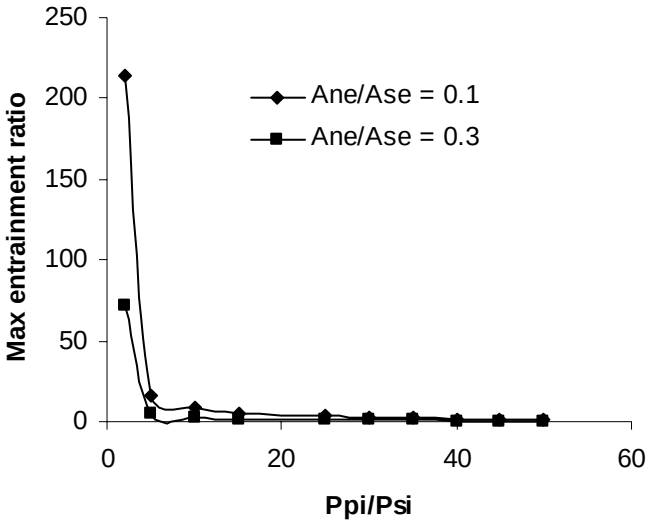

Figure 4: Maximum entrainment ratio variation versus the stagnation pressure ratio for different primary-to-secondary nozzles area ratios (based on $\phi_{inletchoke}$, and ϕ_{Fabri} only)

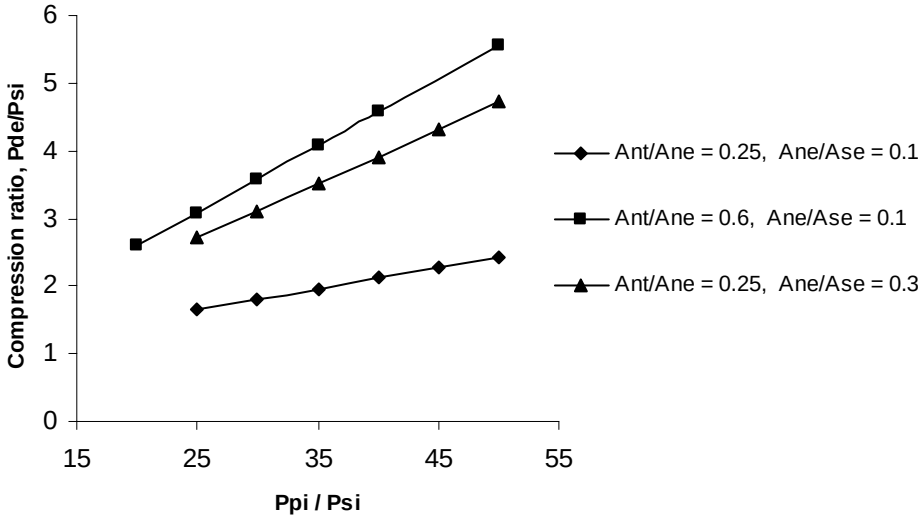

Figure 5: Compression ratio variation versus the stagnation pressure ratio

REFERENCES

Addy, A. L., Dutton, J. C., and Mikkelsen, C.D., 1981, "Supersonic Ejector-Diffuser Theory and Experiments," Report No. UILU-ENG-82-4001, Department of Mechanical and Industrial Engineering, University of Illinois at Urbana-Champaign, Urbana, Illinois, August.

Al-Ansary, H. A. and Jeter, S. M., 2004, "Numerical and Experimental Analysis of Single-Phase and Two-Phase Flow in Ejectors," *HVAC&R Research*, Vol. 10, No. 4, pp. 521-538, October.

Dorantes, R., Estrada, C. A., and Pilatowsky, I., 1996, "Mathematical Simulation of a Solar Ejector-Compression Refrigeration System," *Applied Thermal Engineering*, Vol. 16, pp. 669-675.

Dutton, J. C. and Carroll, B. F., 1988, "Limitations of Ejector Performance Due to Exit Choking," ASME *Journal of Fluids Engineering*, Vol. 110, pp. 91-93, March.

Dutton, J. C. and Carroll, B. F., 1986, "Optimal Supersonic Ejector Designs," ASME *Journal of Fluids Engineering*, Vol. 108, No. 4, pp. 414-420.

Eames, I. W., 2002, “A New Prescription for the Design of Supersonic Jet-Pumps: The Constant Rate of Momentum Change Method,” *Applied Thermal Engineering*, Vol. 22, No. 2, pp. 121-131, February.

Elger, D.F., McLam, E.T., and Taylor, S.J., 1991, “A New Way to Represent Jet Pump Performance,” ASME *Journal of Fluids Engineering*, Vol. 113, No. 3, pp. 439-444.

Fabri, J. and Paulon, J., 1958, “Theory and Experiments on Air-to-Air Supersonic Ejectors,” NACA-TM-1410, September.

Fabri, J. and Siestrunk, R., 1958, “Supersonic Air Ejectors,” Advances in Applied Mechanics, Vol. V, H.L. Dryden and Th. von Karman (editors), Academic Press, New York, pp. 1-33.

Kandil, S., Lear, W.E., and Sherif, S.A., 2003, “Regenerative Jet-Pumped Thermal Management Systems for Spacecraft Mass Reduction,” *41st AIAA Aerospace Sciences Meeting and Exhibit*, Reno, Nevada, January 6-9, AIAA Paper No. AIAA-2003-501.

Kandil, S.M., Lear, W.E., and Sherif, S.A., 2002, "Mass Advantages in a Jet-Pumped Active Thermal Management System," *SAE Transactions-Journal of Aerospace*, Vol. 111, No. 1, pp. 765-773.

Kandil, S.M., Lear, W.E., and Sherif, S.A., 2004, “Performance of a Jet-Pumped Cryogenic Refrigeration System,” AIAA *Journal of Propulsion and Power*, Vol. 20, No. 6, November/December, pp. 1018-1025.

Lear, W.E., Sherif, S.A., Steadham, J.M., 2000, “Design Considerations of Jet Pumps with Supersonic Two-Phase Flow and Shocks for Refrigeration and Thermal Management Applications,” *International Journal of Energy Research*, Vol. 24, pp. 1373-1389.

Lear, W.E., Sherif, S.A., Steadham, J.M., Hunt, P.L., and Holladay, J.B., 1999, “Design Considerations of Jet Pumps with Supersonic Two-Phase Flow and Shocks,” *37th AIAA Aerospace Sciences Meeting*, Reno, Nevada, January 11-14, AIAA Paper 99-0461.

Nord, J.W., Lear, W.E., and Sherif, S.A., 2001, “Analysis of a Heat-Driven Jet-Pumped Cooling System for Space Thermal Management,” *AIAA Journal of Propulsion and Power*, Vol. 17, No. 3, May-June, pp. 566-570.

Parker, G. M., Lear, W. E., and Sherif, S. A., 2001, “On an Optimum Geometry of a Two-Phase Ejector,” *Proceedings of the 36th Intersociety Energy Conversion Engineering Conference*, Savannah, Georgia, July 29-August 2, Paper No. IECEC2001-TM-14, Vol. 2, pp. 1187-1194.

Roan, V.P., 1991, “An Ejector Performance Correlation Factor,” *AIAA 27th Joint Propulsion Conference*, Sacramento, CA, June 24-26, AIAA-91-2545, pp. 1-4.

Sherif, S.A., Lear, W.E., Steadham, J.M., Hunt, P.L., and Holladay, J.B., 2000, “Analysis and Modeling of a Two-Phase Jet Pump of a Thermal Management System for Aerospace Applications,” *International Journal of Mechanical Sciences*, Vol. 42, No. 2, February, pp. 185-198.